Eur Radiol (2006) 16: 256–268
DOI 10.1007/s00330-005-2919-2



# First performance evaluation of a dual-source CT (DSCT) system

**Thomas G. Flohr**
**Cynthia H. McCollough**
**Herbert Bruder**
**Martin Petersilka**
**Klaus Gruber**
**Christoph Süβ**
**Michael Grasruck**
**Karl Stierstorfer**
**Bernhard Krauss**
**Rainer Raupach**
**Andrew N. Primak**
**Axel Küttner**
**Stefan Achenbach**
**Christoph Becker**
**Andreas Kopp**
**Bernd M. Ohnesorge**

Received: 8 November 2005
Accepted: 21 November 2005
Published online: 10 December 2005


T. G. Flohr (✉) · H. Bruder · M. Petersilka · K. Gruber · C. Süβ · M. Grasruck · K. Stierstorfer · B. Krauss · R. Raupach · B. M. Ohnesorge
Siemens Medical Solutions, Computed Tomography CTE PA, Siemensstr. 1, 91301 Forchheim, Germany
e-mail: thomas.flohr@siemens.com
Tel.: +49-9191-188195

T. G. Flohr · A. Kopp
Department of Diagnostic Radiology, Eberhard-Karls-Universität Tübingen, Tübingen, Germany

C. H. McCollough · A. N. Primak
Mayo Clinic College of Medicine, Department of Radiology, Rochester, MN, USA

A. Küttner
Department of Diagnostic Radiology, Friedrich-Alexander-Universität Erlangen, Erlangen, Germany

S. Achenbach
Department of Cardiology, Friedrich-Alexander-Universität Erlangen, Erlangen, Germany

C. Becker
Department of Diagnostic Radiology, Klinikum Groβhadern, Ludwigs-Maximilians-Universität München, München, Germany

**Abstract** We present a performance evaluation of a recently introduced dual-source computed tomography (DSCT) system equipped with two X-ray tubes and two corresponding detectors, mounted onto the rotating gantry with an angular offset of 90°. We introduce the system concept and derive its consequences and potential benefits for echocardiograph (ECG)-controlled cardiac CT and for general radiology applications. We evaluate both temporal and spatial resolution by means of phantom scans. We present first patient scans to illustrate the performance of DSCT for ECG-gated cardiac imaging, and we demonstrate first results using a dual-energy acquisition mode. Using ECG-gated single-segment reconstruction, the DSCT system provides 83 ms temporal resolution independent of the patient's heart rate for coronary CT angiography (CTA) and evaluation of basic functional parameters. With dual-segment reconstruction, the mean temporal resolution is 60 ms (minimum temporal resolution 42 ms) for advanced functional evaluation. The z-flying focal spot technique implemented in the evaluated DSCT system allows 0.4 mm cylinders to be resolved at all heart rates. First clinical experience shows a considerably increased robustness for the imaging of patients with high heart rates. As a potential application of the dual-energy acquisition mode, the automatic separation of bones and iodine-filled vessels is demonstrated.

**Keywords** Computed tomography · Cardiac CT · CT technology · Dual-source CT · Multidetector-row CT

## Introduction

### Current status of ECG-gated cardiac CT

Echocardiograph (ECG)-gated cardiac computed tomography (CT) examinations with multidetector-row CT (MDCT) systems were introduced in 1999 [1–3]. Early yet promising results with this new technique paved the way for the ongoing integration of coronary CT angiography (CTA) into routine clinical algorithms. The temporal resolution of 250 ms with the first-generation of four-slice systems was sufficient for motion-free imaging of the heart in the mid- to end-diastolic phase at slow to moderate heart rates (i.e., up to 65 bpm, [4]). With four simultaneously acquired slices, coverage of the entire heart volume with thin slices (i.e., 4×1 mm or 4×1.25 mm collimation) within a single breath hold became feasible. This 1- to 1.25-mm longitudinal resolution combined with the improved contrast resolution of modern CT systems enabled noninvasive visualization of the coronary arteries [5–8]. The initial clinical studies demonstrated MDCT's potential to not only detect but to some degree also characterize noncalcified and calcified plaques in the coronary arteries based on their CT attenuation [9, 10]. With regard to the quantification of calcium (Ca) in the coronary arteries (Ca scoring), comparative studies of electron-beam CT (EBCT) and prospectively ECG-triggered four-slice CT were performed that could demonstrate good agreement of the measurements in phantom experiments [11] and high correlation in patient studies [12]. Early experience demonstrated that basic cardiac function parameters derived with four-slice CT correlate well with the gold-standard techniques of magnetic resonance imaging (MRI) and coronary angiography based on a standardized selection of the cardiac phase for end-diastolic and end-systolic CT reconstruction and semiautomated evaluation tools [13]. Despite all these promising advances, challenges and limitations with respect to motion artifacts in patients with higher heart rates, limited spatial resolution, and long breath-hold times remained for four-slice cardiac CT. Stents or severely calcified arteries constitute a diagnostic dilemma using these systems, mainly due to partial volume artifacts as a consequence of insufficient longitudinal resolution [8]. For patients with higher heart rates, careful selection of separate reconstruction intervals for different coronary arteries has been mandatory [14]. The breath-hold time of about 40 s required to cover the entire heart volume (~12 cm) with four-slice CT is almost impossible to comply with for patients with manifest heart disease.

Sixteen-slice CT systems with gantry rotation times down to 0.375 s have improved spatial and temporal resolution compared to four-slice scanners while examination times are considerably reduced: the entire heart volume can be covered with submillimeter slices in 15–20 s [15, 16]. Sixteen-slice systems have been used to introduce ECG-triggered and ECG-gated MDCT examinations of the heart and the coronary arteries into clinical practice. Detection and characterization of coronary plaques, even in the presence of severe calcifications, benefit from the increased robustness of 16-slice technology. A study of coronary CTA with a 16-slice system in 59 patients demonstrated 86% specificity and 95% sensitivity for identifying significant coronary artery stenosis. None of the patients had to be excluded [17], as in previous studies, based on less-advanced scanner technology. Other investigators reported similar results [18–20].

The latest generation of 64-slice CT systems provides further increased spatial resolution (0.4-mm isotropic voxels with the use of advanced z-sampling techniques [21]) and improved temporal resolution due to gantry rotation times down to 0.33 s, and they are a further leap in integrating coronary CTA into routine clinical algorithms. ECG-gated cardiac scanning benefits from both improved temporal resolution and improved spatial resolution. Nevertheless, motion artifacts remain the most important challenge for coronary CTA, even with the latest generation of MDCT. While image quality at higher heart rates and robustness of the method in clinical routine seem to be significantly improved with 64-slice CT systems compared with previous generations of MDCT systems, several authors still propose the administration of beta-blockers. Leber et al. included the oral administration of 50 mg of metoprolol into their study protocol for patients with heart rates >70 bpm [22]. Raff et al. reported excellent specificity, sensitivity, and positive and negative predictive values of 95%, 90%, 93%, and 93%, respectively, for the presence of significant stenosis on a per-patient basis [23]. Patients in this study received medication with atenolol to achieve a target heart rate <65 bpm, yet no patient was excluded because of a heart rate above this target. Mollet et al. reported similar results for their study group who received beta-blockers if the initial heart rate was >70 bpm [24]. Even though Wintersperger et al. demonstrated the ability of 64-slice CT with a gantry rotation time of 0.33 s to produce diagnostic image quality over a wide range of heart rates (up to 92 bpm) with a low number of nondiagnostic segments, even at high heart rates [25], some heart rates are still problematic. The authors observed good image quality in diastole for patients with heart rates <65 bpm and good image quality in end systole for patients with heart rates >75 bpm, yet image quality in the intermediate region was compromised, and neither diastolic nor systolic reconstruction yielded optimal results reliably.

### Potential for improvement and alternative system concepts

Further-improved temporal resolution of less than 100 ms at all heart rates is desirable to completely eliminate the need for heart-rate control. Increased gantry rotation speed

rather than multisegment reconstruction approaches appears preferable for robust clinical performance [26]. Obviously, significant development efforts are needed to account for the substantial increase in mechanical forces (~17G for 0.42 s rotation time, ~28G for 0.33 s rotation time) and increased data transmission rates. Rotation times of less than 0.2 s (mechanical forces >75G), which are required to provide a temporal resolution of less than 100 ms independent of the heart rate, appear to be beyond today's mechanical limits.

An alternative scanner concept that avoids any mechanically moving parts is the EBCT. An electron beam is emitted from a powerful electron gun and magnetically deflected to hit a semicircular anode surrounding the patient. The magnetic deflection sweeps the electron beam over the target, thus generating an X-ray source that virtually rotates around the patient. Given the absence of mechanically moving parts, a sweep can be accomplished in as little as 50 ms.

EBCT systems were already introduced in 1984 as a noninvasive imaging modality for the diagnosis of coronary artery disease [27–30]. The technical principles have been discussed previously [31–33]. Due to the restriction to nonspiral, sequential scanning, a single breath-hold scan of the entire heart requires slice widths not smaller than 3 mm. The resulting limited longitudinal resolution is sufficient for Ca-scoring examinations; it is, however, not adequate for 3-D visualization of the coronary arteries. EBCT suffers from inherent disadvantages of the measurement principle, which have prevented a more wide-spread use of these systems in cardiology or general radiology. Due to the fourth-generation system geometry, the use of anti-scatter collimator blades on the detector is not possible. As a consequence, image quality is degraded by scattered radiation, with typical artifacts presenting, e.g., in the form of hypodense zones in the mediastinum. Due to the ring collimator used to shape the beam in the z-direction, the radiation profiles on the detector are "banana shaped," resulting in a problematic geometrical dose efficiency of the system. While the available X-ray power is sufficient for small patients, it is at the limit for medium-sized and larger patients. As a consequence, signal-to-noise ratio is at least problematic, if not insufficient, for larger patients. In summary, the EBCT principle is currently not considered adequate for state-of-the-art cardiac imaging or for general radiology applications.

An alternative concept to improve temporal resolution for cardiac CT while maintaining the good general imaging capabilities of a modern third-generation CT system is a scanner design with multiple X-ray sources and detectors that has already been described in the early times of CT [34, 35]. In this paper, we evaluate a recently introduced dual-source CT (DSCT) system (SOMATOM Definition, Siemens Medical Solutions, Forchheim, Germany). We introduce the system concept and derive its consequences and potential benefits for ECG-controlled cardiac CT and for general radiology applications. We evaluate both temporal and spatial resolution by means of phantom scans. We present first patient scans to illustrate the performance of DSCT for ECG-gated cardiac imaging, we demonstrate first results using a dual-energy acquisition mode, and we end with a discussion of the potential of DSCT for both cardiac and general-purpose CT.

## Materials and methods

### Instrumentation

#### *DSCT system design*

The evaluated DSCT system is equipped with two X-ray tubes and two corresponding detectors. The two acquisition systems are mounted onto the rotating gantry with an angular offset of 90°. Figure 1 illustrates the principle. One detector (A) covers the entire scan field of view (50 cm in diameter) while the other detector (B) is restricted to a smaller, central field of view (26 cm in diameter) due to space limitations on the gantry (see Fig. 2). Each detector comprises 40 detector rows, the 32 central rows having a 0.6-mm collimated slice width and the outer rows on both sides having a 1.2-mm collimated slice width. The total coverage in the longitudinal direction (z-direction) of each detector is 28.8 mm at isocenter. By proper combination of the signals of the individual detector rows, the detector configurations of 32×0.6 mm or 24×1.2 mm can be realized. Using the z-flying focal spot technique [21, 36], two subsequent 32-slice readings with 0.6 mm collimated slice width are combined to one 64-slice projection with a

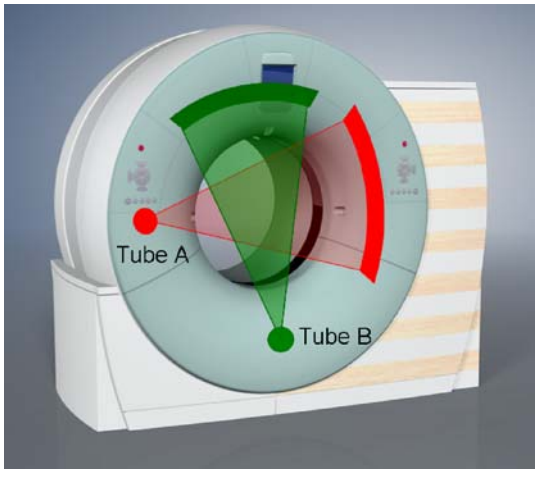


**Fig. 1** The evaluated dual-source computed tomography (DSCT) system with a schematic illustration of the acquisition principle using two tubes and two corresponding detectors offset by 90°. A scanner of this type provides temporal resolution equivalent to a quarter of the gantry rotation time, independent of the patient's heart rate

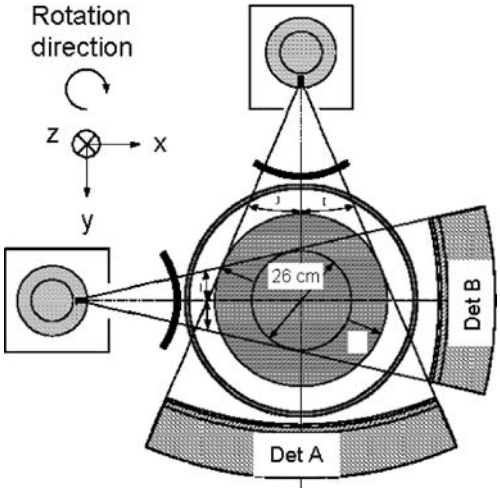


**Fig. 2** Technical realization of the dual-source computed tomography (DSCT) system. One detector (*A*) covers the entire scan field of view with a diameter of 50 cm while the other detector (*B*) is restricted to a smaller, central field of view due to space limitations on the gantry

sampling distance of 0.3 mm at isocenter. In this way, each detector acquires 64 overlapping 0.6 mm slices per rotation. The shortest gantry rotation time is 0.33 s; other gantry rotation times are 0.5 s and 1.0 s. Each of the two rotating envelope X-ray tubes (STRATON, Siemens Medical Solutions, Forchheim, Germany, [37]) allows up to 80-kW peak power from the two on-board generators. Both tubes can be operated independently with regard to their kilovolt (kV) and milliampere (mA) settings. This allows the acquisition of dual-energy data, with one tube being operated at, e.g., 80 kV while the other is operated at, e.g., 140 kV.

### *Key features of DSCT for ECG-gated cardiac scanning*

The key benefit of DSCT for cardiac scanning is improved temporal resolution. A scanner of this type provides temporal resolution of approximately a quarter of the gantry rotation time, independent of the patient's heart rate and without the need for multisegment reconstruction techniques. In general, partial scans are used for ECG-gated image reconstruction with single-source CT systems, with a scan data segment covering 180° plus the detector fan angle (about 50–60°, depending on system geometry). This is the minimum data necessary for image reconstruction throughout the entire scan field of view (SFOV) of usually 50-cm diameter. The temporal resolution at a certain point in the SFOV is determined by the acquisition time window of the data, contributing to the reconstruction of that particular image point. Similar to slice-sensitivity profiles (SSP), temporal resolution may be characterized by time-sensitivity profiles (TSP). The temporal resolution $\Delta T_{ima}$ assigned to an image is the full width at half maximum (FWHM) of the TSP. In a single-source, noncardiac partial scan approach, the entire partial scan data segment is used for image reconstruction at any point of the SFOV. Redundant data are weighted using algorithms such as the one described by Parker [38]. To improve temporal resolution, modified reconstruction approaches for partial scan data have been proposed [1, 39], which are best explained in parallel geometry. A third-generation CT scanner acquires data in fan-beam geometry, characterized by the projection angle α and by the fan angle β within a projection. Another set of variables serving the same purpose is θ and b: θ is the azimuthal angle and b denotes the distance of a ray from the isocenter (see Fig. 3), and θ and b are used to label rays when projection data are in the form of parallel projections. A simple coordinate transformation relates the two sets of variables.

$$\theta = \alpha + \beta \tag{1}$$

and

$$b = R_F \sin\beta \tag{2}$$

where $R_F$ is the focus-isocenter distance of the scanner. Using these equations, the measured fan-beam data can be transformed to parallel data, a procedure called "rebinning." In parallel geometry, 180° of scan data—a half-scan sinogram—are necessary for image reconstruction. Due to data acquisition in fan-beam geometry, a partial

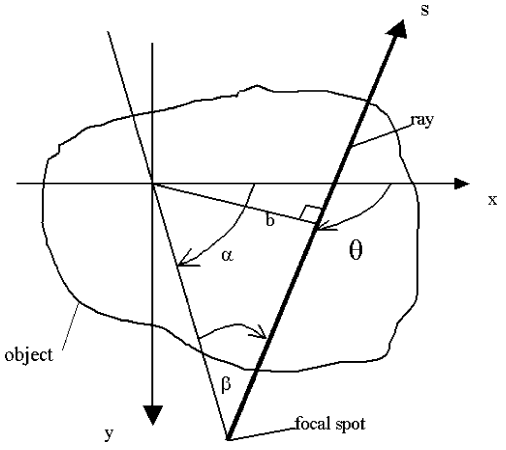


**Fig. 3** Definition of variables used to characterize the measurement rays of a computed tomography (CT) scanner. A parallel projection is obtained by assembling rays from several fan-beam projections

scan interval larger than 180°, namely, 180° plus the detector fan angle, is necessary to provide 180° of parallel data for any image point within the SFOV. In the center of rotation, for β=0, 180° of the acquired fan-beam data are sufficient to provide 180° of parallel data (see Eq. 1). If all redundant data are neglected, temporal resolution $\Delta T_{ima}$in the center of rotation can be as good as 180°/360°=1/2 times the rotation time of a single-source CT scanner. For 0.33 s rotation $\Delta T_{ima}=t_{rot}/2=165$ ms.

In a DSCT scanner, the half-scan sinogram in parallel geometry can be split up into two quarter-scan sinograms, which are simultaneously acquired by the two acquisition systems in the same relative phase of the patient's cardiac cycle and at the same anatomical level due to the 90° angle between both detectors (see Fig. 4). The two quarter-scan segments are appended by means of a smooth transition function to avoid streaking or other artifacts from potential discontinuities at the respective start and end projections (transition angle 30°). The use of a transition function does not affect the FWHM of the TSP. Since the second detector does not cover the entire SFOV, its projections are potentially truncated and have to be extrapolated by using data acquired with the first detector at the same projection angle (i.e., a quarter rotation earlier). With this approach, constant temporal resolution $\Delta T_{ima}$ equivalent to a quarter of the gantry rotation time $t_{rot}/4$ is achieved in a centered region of the scan field of view that is covered by both acquisition systems. For $t_{rot}=0.33$ s, the temporal resolution is $\Delta T_{ima}=t_{rot}/4 = 83$ ms, independent of the patient's heart rate. Data from one cardiac cycle only are used to reconstruct an image. Thus, the basic mode of operation of a DSCT system corresponds to single-segment reconstruction. This is a major difference to conventional MDCT systems, which can theoretically provide similar temporal resolution by means of multisegment reconstruction approaches [39, 2]. With these approaches, temporal resolution strongly depends on the heart rate, and a stable and predictable heart rate and complete periodicity of the heart motion are required for adequate performance. Optimal temporal resolution can only be achieved at a few "sweet spots," where the patient's heart rate and the gantry rotation time of the scanner are properly desynchronized.

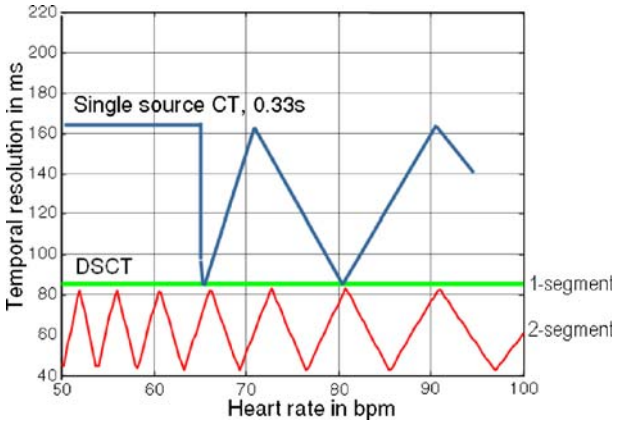


**Fig. 5** Temporal resolution as a function of the patient's heart rate for a single-source multidetector-row computed tomography (MDCT) system at 0.33-s gantry rotation time and for the evaluated dual-source CT (DSCT) scanner at 0.33-s gantry rotation time. The MDCT reaches 83 ms temporal resolution only using dual-segment reconstruction and only at 66 bpm, 81 bpm, and 104 bpm (*blue line*). The DSCT system provides 83 ms temporal resolution independent of the patient's heart rate using single-segment reconstruction (*green line*). Using dual-segment reconstruction (*red line*), temporal resolution varies as a function of the heart rate, and a mean temporal resolution of about 60 ms can be established for advanced functional evaluations

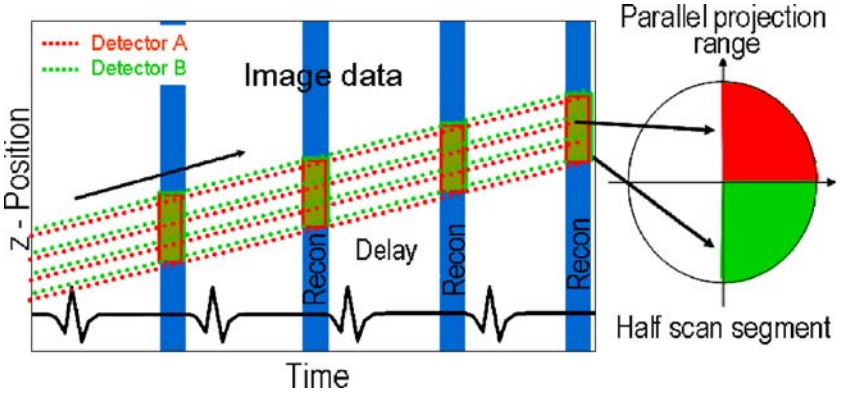


**Fig. 4** Principle of echocardiograph (ECG)-gated spiral image reconstruction for a dual-slice computed tomography (DSCT) system. The position of the detector slices of both measurement systems A (*red dotted lines*) and B (*green dotted lines*) relative to the patient is indicated as a function of time. At the bottom, the patient's ECG signal is shown schematically. To simplify the drawing, only four detector slices are shown, and the red and green lines are slightly shifted in the z-direction. In reality, each of the two detectors in the evaluated DSCT scanner acquires 64 overlapping 0.6-mm slices by means of double z-sampling. Both detectors cover the same z-positions; there is no z-shift between them. Due to the 90° angle between both detectors, the half-scan sinogram in parallel geometry can be split up into two quarter-scan sinograms, which are simultaneously acquired by the two acquisition systems in the same relative phase of the patient's cardiac cycle and at the same anatomical level (indicated as *red and green quarter circles*)

Figure 5 shows the temporal resolution as a function of the patient's heart rate for a conventional MDCT system with 0.33-s gantry rotation time (SOMATOM Sensation 64, Siemens Medical Solutions, Forchheim, Germany) and for the evaluated DSCT system. While the MDCT reaches 83 ms temporal resolution only using dual-segment reconstruction and only at 66 bpm, 81 bpm, and 104 bpm, the DSCT provides 83 ms temporal resolution at all heart rates using only one cardiac cycle worth of data.

It is interesting to note that multisegment approaches can also be applied to DSCT. In a two-segment reconstruction, the quarter-scan segments acquired by each of the two detectors are independently divided into smaller subsegments acquired in subsequent cardiac cycles of the patient—similar to two-segment reconstruction in conventional MDCT. Using a multisegment approach, temporal resolution again varies as a function of the patient's heart rate, and a mean temporal resolution of about 60 ms can be established at 0.33-s gantry rotation time (see Fig. 5) (minimum temporal resolution 42 ms). While this mode is not recommended for coronary angiography examinations, it may be beneficial for advanced functional evaluations, such as the detection of wall motion abnormalities, or the determination of parameters, such as peak ejection fraction. For coronary angiography examinations and the assessment of basic functional parameters, the single-segment mode is expected to provide sufficient temporal resolution at clinically relevant heart rates.

Since multisegment reconstruction for higher heart rates will not be required for coronary CTA and basic functional evaluation, the table feed can be efficiently adapted to the patient's heart rate and significantly increased at elevated heart rates. It has been shown [39] that the pitch, $p$, for a single-segment ECG-gated spiral reconstruction should not exceed

$$p = \left(\frac{M-1}{M}\right)\frac{t_{rot}}{T_{RR}} \tag{3}$$

for gapless volume coverage in any phase of the cardiac cycle. $M$ is the number of collimated detector rows, $t_{rot}$ is the gantry rotation time, and $T_{RR}$ is the patient's heart cycle time. For the evaluated DSCT system, $M$=32 and $t_{rot}$=0.33 s. In terms of the heart rate (heart rate HR= $60/T_{RR}$, in beats/minute bpm) and assuming a confidence interval of 10 bpm that the heart rate of the patient is allowed to drop during examination, the allowed pitch and table feed settings may be calculated (Table 1).

Using the evaluated CT scanner, the heart rate of the patient is monitored before the examination, the lowest heart rate observed during the monitoring phase is taken, and an additional safety margin of 10 bpm is subtracted to automatically adjust the table feed for the scan. The safety margin of 10 bpm is already included in the values shown in Table 1.

**Table 1** Heart-rate-dependent pitch and table feed settings for the evaluated dual-slice computed tomography (DSCT) scanner

| Heart rate in bpm | Pitch | Table feed in mm/s |
|---|---|---|
| 50 | 0.21 | 12.8 |
| 60 | 0.27 | 16.0 |
| 70 | 0.32 | 19.2 |
| 80 | 0.37 | 22.4 |
| 90 | 0.43 | 25.6 |

The increased pitch at higher heart rates does not only reduce the examination time but reduces the radiation dose to the patient. With a single-source CT, the pitch cannot be increased at higher heart rates because multisegment reconstruction must be used to improve temporal resolution. This is not necessary for DSCT. Another means to reduce patient dose, which is implemented in the evaluated DSCT scanner, is a flexible ECG-pulsing mechanism, which reacts to ectopic beats and heart rate variations.

### *Key features of DSCT for general radiology applications*

Using only one of the two acquisition systems, the evaluated DSCT scanner is a fully functional, 64-slice, single-source CT for general radiology applications. Its performance is essentially the same as previously described [36]. If both acquisition systems are used, DSCT systems show some interesting properties for general radiology applications in addition to the benefit of improved temporal resolution for cardiac CT examinations.

First, both X-ray tubes can be operated simultaneously in a standard spiral or sequential acquisition mode, in this way providing up to 160 kW X-ray peak power. Additionally, both X-ray tubes can be operated at different kV and mA settings, allowing the acquisition of dual-energy data. While dual-energy CT was evaluated 20 years ago [40, 41], technical limitations of the CT scanners at those times prevented the development of routine clinical applications. For a successful application of dual-energy postprocessing algorithms, the image noise in both image data sets—acquired at low kV (e.g., 80 kV) and at high kV (e.g. 140 kV)—has to be similar, which was not possible in the early days of dual-energy CT due to insufficient power reserves for the low kV scan. This limitation no longer exists on the DSCT system, and dual-energy data can be acquired nearly simultaneous with subsecond scan times. The ability to overcome data registration problems should provide clinically relevant benefits.

The use of dual-energy CT data can in principle add functional information to the morphological information based on X-ray attenuation coefficients that is usually obtained in a CT examination. A potential application is the separation of bones and iodine-filled vessels in CT angi-

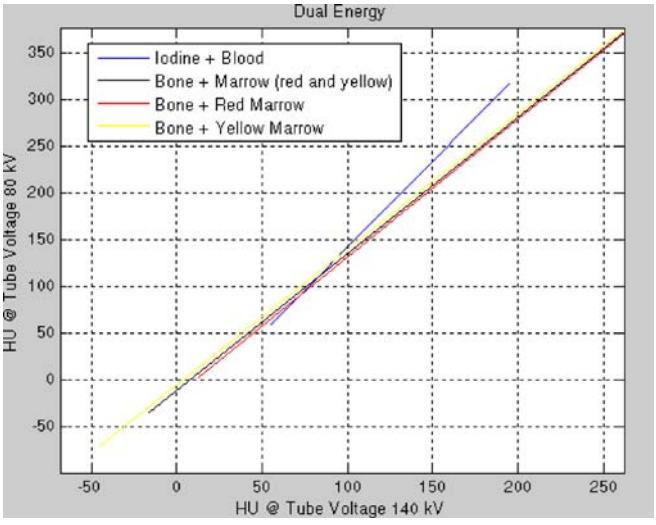


**Fig. 6** Computer simulation of the computed tomography (CT) values (HU) of mixtures of iodine and blood and of bone and bone marrow at X-ray tube voltages of 80 kV and 140 kV, illustrating the potential of dual-energy CT to separate image pixels with a CT value >100 HU at 140 kV into iodine pixels (*blue line*) or bone pixels (*black*, *red*, and *yellow lines*) according to their position in the diagram

ographic examinations, e.g., of the circle of Willis, so that the bones can be automatically removed with only the vessels remaining in the resultant images. Iodine shows a much larger increase of the CT value with decreasing X-ray tube voltage than hydroxyapatite, which is the basis for iodine–bone separation using dual-energy CT. Figure 6 shows a computer simulation of the CT values of mixtures of iodine and blood and of bone and bone marrow at X-ray tube voltages of 80 kV and 140 kV, using the prefiltration of the evaluated DSCT scanner. In principle, image pixels with a CT value >100 HU at 140 kV should be separable into iodine pixels or bone pixels according to their position in the diagram of Fig. 6. The quality of the separation will improve with increasing CT density. At low to medium CT values, it will be hampered by image noise, requiring the use of additional knowledge-based postprocessing algorithms to reliably identify the corresponding pixels.

## Phantom experiments

### *Evaluation of temporal resolution*

We performed experiments with a moving coronary artery phantom to compare the performance of the evaluated DSCT and a state-of-the-art MDCT (SOMATOM Sensation 64, Siemens Medical Solutions, Forchheim, Germany) for ECG-gated spiral scanning, in particular with regard to temporal resolution. The phantom consisted of three contrast-filled lucite tubes with a lumen of 4 mm. Coronary artery stents were inserted in two of the tubes. One of the stents contained an artificial 50% stenosis. The tubes were immersed in a water bath and moved in a periodic manner by a computer-controlled robot arm at an angle of 45° relative to the scan plane to simulate heart motion (see Fig. 7). The motion amplitudes and velocities of the robot arm were based on published values for the coronary arteries (42) to provide a model as realistic as possible. We scanned the phantom with the DSCT scanner and the single-source 64-slice CT. We used motion patterns corresponding to heart rates of 70 bpm and 90 bpm. Figure 8 shows the motion curve for 90 bpm. Scan parameters for the DSCT system were: 120 kV, 400 mA for each X-ray tube, 0.33-s gantry rotation, 32×0.6 mm collimation for each detector, pitch 0.32 (70 bpm) and pitch 0.43 (90 bpm), and single-segment reconstruction with 83-ms temporal resolution. For the MDCT, we used the standard protocol for ECG-gated coronary CTA: 120 kV, 500 mA, 0.33-s gantry rotation, 32×0.6-mm collimation, pitch 0.2, and two-segment reconstruction with ~140 ms and ~160 ms temporal resolution at 70 bpm and 90 bpm, respectively. For both systems, the z-flying focal spot technique was used to acquire 64 simultaneous overlapping 0.6-mm slices [21].

### *Measurement of slice-sensitivity profiles (SSPs)*

To determine SSPs for the ECG-gated spiral mode of the DSCT system, we scanned a thin gold plate (40-μm thick) embedded in a lucite cylinder. The gold plate was placed

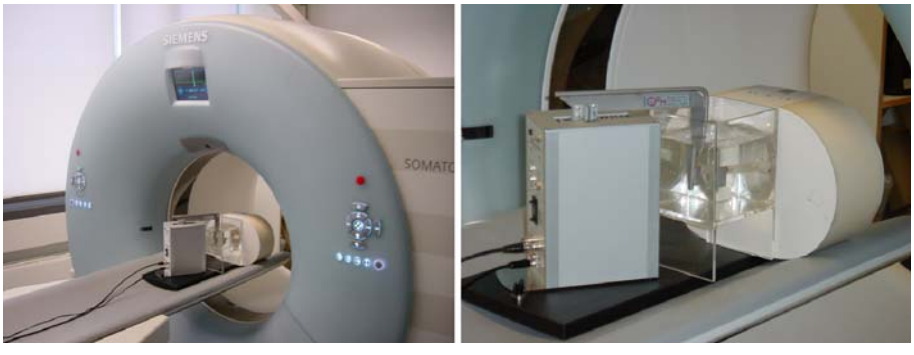


**Fig. 7** Computer-controlled robot arm moving contrast-filled tubes ("coronary arteries") in a water tank. The motion amplitudes and velocities of the robot arm can be adjusted to provide a realistic motion pattern of the coronary arteries

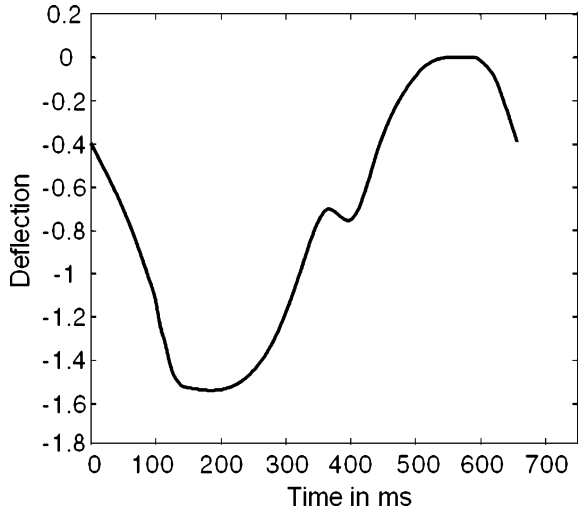


**Fig. 8** Example of a motion curve for the computer-controlled robot arm, simulating a heart rate of 90 bpm. Shown is the motion pattern of a coronary artery based on values given in the literature

close to the isocenter of the scanner, and highly overlapping images with an increment of 0.1 mm were reconstructed for the desired nominal slice widths. The reconstruction range was large enough to encompass the SSP of the system, i.e., in the first and last images, the gold plate had completely disappeared, and only the lucite cylinder was visible. For each of the overlapping images, the mean CT value in a small region of interest within the gold plate was determined, and the background CT value (CT value of the lucite cylinder without the gold plate) was subtracted. The maximum of these corrected mean values (with the gold plate fully in the reconstructed slice) was normalized to 1. The normalized mean values, plotted as a function of the z-positions of the respective image slices, represent the measured SSP. The FWHM of this SSP is the measured slice width. The scan parameters were: 120 kV, 200 mA for each X-ray tube, 0.33-s gantry rotation, 32×0.6-mm collimation for each detector (with z-flying focal spot), pitch 0.32, and single-segment reconstruction with 83-ms temporal resolution. Using an artificial ECG signal with 70 bpm, we reconstructed overlapping images with 0.6-mm, 0.75-mm, 1.0-mm, 1.5-mm, and 2-mm nominal slice width and 0.1-mm increment.

*Investigation of longitudinal (z-axis) spatial resolution*

To investigate the maximum achievable longitudinal resolution of the DSCT system for ECG-gated spiral scanning, we scanned a z-resolution phantom placed at the isocenter of the scanner. The z-resolution phantom consists of a lucite plate with rows of cylindrical holes (diameters 0.4 mm, 0.5 mm, 0.6 mm, 0.7 mm, 0.8 mm, 0.9 mm, 1.0 mm, 1.2 mm, 1.5 mm, 2 mm, and 3 mm) aligned in the z-direction. The scan parameters for the DSCT system were: 120 kV, 250 mA for each X-ray tube, 0.33-s gantry rotation, 32×0.6-mm collimation for each detector (with z-flying focal spot), pitch 0.32 (70 bpm) and pitch 0.43 (90 bpm), and single-segment reconstruction with 83-ms temporal resolution. We reconstructed overlapping images with 0.6-mm nominal slice width and 0.1-mm increment and used multiplanar reformations (MPRs) in the z-direction to determine the minimum diameter of the cylinders that could be resolved and to evaluate geometrical distortions.

*Investigation of dual-energy imaging*

For a first investigation of the dual-energy imaging capabilities of the evaluated DSCT scanner, we scanned a piece of pork containing bone and metal pieces. Tubes filled with solutions of contrast agent with different densities were wrapped around it and put through holes in the bone. The whole specimen was inserted into a water tank with a diameter of 20 cm. The goal of the experiment was the separation of bone and iodine using dual-energy information. Scan parameters were: 140 kV and 150 mA (tube A), 80 kV and 350 mA (tube B), 0.5-s gantry rotation, and 32×0.6-mm collimation with z-flying focal spot for each detector.

Patient examinations

Patients referred for clinically indicated CT coronary angiography were imaged using the evaluated DSCT scanner. A group of eight patients were scheduled for coronary CTA and did not receive medication to lower the heart rate prior to the examination. Six patients had stable heart rates during the scan (variation not larger than ±5 bpm), namely, 65 bpm, 90 bpm, 75 bpm, 85 bpm, 90 bpm, and 90 bpm, respectively. The other two patients had varying heart rates, namely, 55 –71 bpm in both cases. The patients received 80–100 ml contrast agent at a flow rate of 4–5 ml/s, followed by a 50-ml saline bolus at the same flow rate. All patients were scanned in craniocaudal direction. The scan parameters were: 120 kV, 550 mA for each X-ray tube, 0.33-s gantry rotation, 32×0.6-mm collimation with z-flying focal spot for each detector, pitch 0.265–0.36, depending on the patient's heart rate, and single-segment reconstruction with 83-ms temporal resolution. The patient's ECG signal was recorded during scan acquisition. The cardiac phase was individually selected for each patient as the phase that produced the best image quality. ECG-based modulation of the tube current was used to lower the radiation exposure in all cases.

## Results

### Phantom experiments

#### *Temporal resolution*

Figures 9 and 10 show axial slices and MPRs of the moving coronary artery phantom at 70 bpm (Fig. 9) and at 90 bpm (Fig. 10), both for the evaluated DSCT system (top) and for a comparable 64-slice single-source CT system (bottom). The temporal resolution of the DSCT is 83 ms in both cases, the temporal resolution of the single source CT with 0.33-s gantry rotation time, and two-segment reconstruction is 140 ms (70 bpm) and 160 ms (90 bpm), respectively. The phantom simulates realistic coronary artery motion, see Fig. 8for a representative motion curve. The images at 70 bpm show only slight motion artifacts with the single-source CT since its temporal resolution (140 ms) is sufficient to adequately visualize the moving phantom if the reconstruction phase is carefully optimized. At 90 bpm, the single-source CT images show increased motion artifacts. Image quality is degraded by blurring, step, and band artifacts as a consequence of the insufficient temporal resolution of 160 ms at this heart rate. With the DSCT system, the depiction of the moving coronary artery phantom is nearly free of artifacts both at 70 bpm and at 90 bpm, thereby allowing for a reliable evaluation of the in-stent lumen at both heart rates.

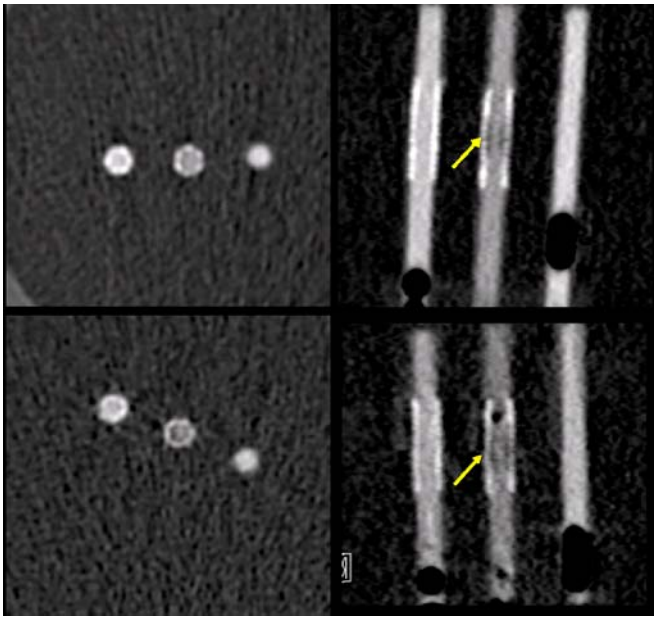

**Fig. 9** Axial slices and multiplanar reformations (MPRs) of the moving coronary artery phantom at 70 bpm for the evaluated dual-source computed tomography (DSCT) system (*top*) and for a comparable 64-slice single-source CT system (*bottom*), both at 0.33-s gantry rotation time. The temporal resolution of the DSCT is 83 ms, and the temporal resolution of the multidetector-row CT (MDCT) using two-segment reconstruction at 70 bpm is 140 ms. The in-stent stenosis (*arrow*) can be clearly appreciated on the DSCT images

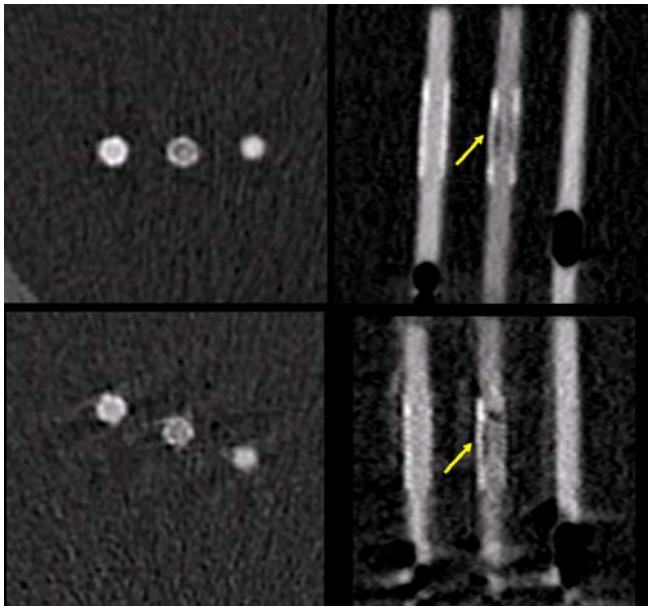

**Fig. 10** Axial slices and multiplanar reformations (MPRs) of the moving coronary artery phantom at 90 bpm for the evaluated dual-source computed tomography (DSCT) system (*top*) and for a comparable 64-slice single-source CT system (*bottom*), both at 0.33-s gantry rotation time. The temporal resolution of the DSCT is 83 ms, and the temporal resolution of the multidetector-row CT (MDCT) using two-segment reconstruction at 90 bpm is 160 ms. The in-stent stenosis (*arrow*) can be clearly appreciated on the DSCT images, the MDCT images show blurring and band artifacts

#### *Slice-sensitivity profiles (SSPs)*

Figure 11 shows measured SSPs (at isocenter) of the nominal 0.6-mm, 0.75-mm, 1.0-mm, 1.5-mm, and 2.0-mm slices for the ECG-gated spiral scan mode of the evaluated DSCT system. The images were reconstructed using an artificial ECG signal with 70 bpm. The reconstruction phase was 60%. The SSPs are symmetrical, bell-shaped curves without far-reaching tails that would degrade longitudinal resolution. The measured FWHMs are 0.7 mm, 0.83 mm, 1.05 mm, 1.5 mm, and 2.05 mm, respectively, in good agreement with the nominal values.

#### *Longitudinal (z-axis) spatial resolution*

Figure 12 shows MPRs of the z-resolution phantom (lucite plate with cylindrical holes) in the isocenter of the DSCT scanner, reconstructed with 0.6-mm nominal slice width (measured FWHM ~0.7 mm) and 0.1-mm image increment. ECG-gated spiral scan data were acquired at pitch $p$=0.32 and $p$=0.43 and reconstructed using artificial

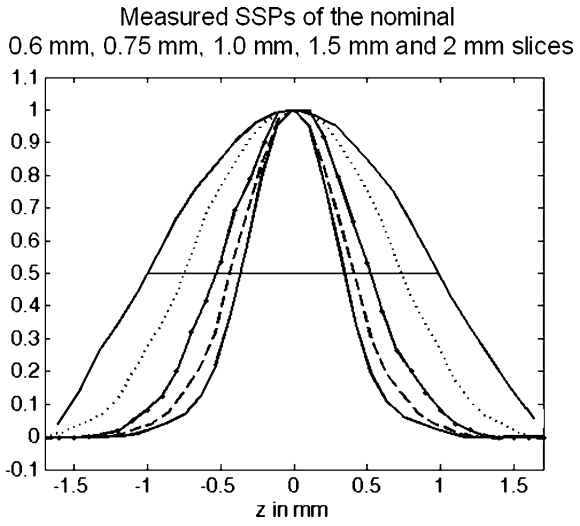


**Fig. 11** Measured slice-sensitivity profiles (SSPs) (at isocenter) of the nominal 0.6 mm, 0.75 mm, 1.0 mm, 1.5 mm, and 2.0 mm slices for the echocardiograph (ECG)-gated spiral scan mode of the evaluated dual-source computed tomography (DSCT) system. The measured full width at half maximums (FWHMs) are 0.7 mm, 0.83 mm, 1.05 mm, 1.5 mm, and 2.05 mm

ECG signals with 70 bpm (Fig. 12, top) and 90 bpm (Fig. 12, bottom), respectively. For both heart rates, all cylinders down to 0.4-mm diameter can be resolved, and the MPRs are free of geometric distortions, thus proving the spatial integrity of the 3-D image. Heart-rate-independent spatial resolution is an important requirement for clinically reliable coronary CTA. Using the thinnest slice width and sharp kernels, 0.5-mm in-plane and 0.4-mm through-plane resolution can be achieved in clinical routine with ECG-gated spiral modes. Using medium-smooth convolution kernels and a nominal 0.75-mm slice to balance resolution and image noise, spatial resolution can be as good as 0.6–0.7 mm in-plane and 0.5 mm through-plane.

### *Investigation of dual-energy CT*

Figure 13 shows the result of the dual-energy specimen study where a contrast-filled tube was wrapped around a pig bone and scanned using 80 kV/140 kV. On the left, the original image is shown. For the image on the right, the bone was automatically removed using dual-energy information. Even in critical anatomical situations where the contrast-filled tubes pass through the bone or are immediately adjacent to it, the fully automated bone–iodine separation was successful.

## Patient examinations

Clinically diagnostic image quality could be obtained for each of the eight patients in our study. In all cases, the coronary arteries were depicted smoothly without the blurring, step, or band artifacts that indicate insufficient tem-

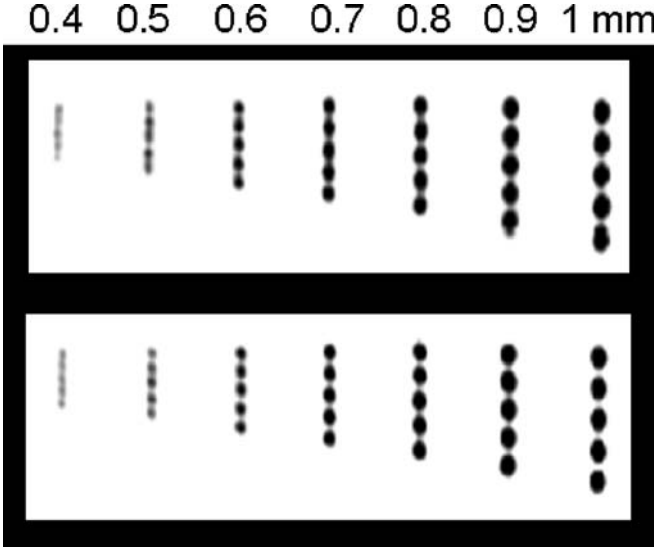


**Fig. 12** Multiplanar reformations (MPRs) of the z-resolution phantom (lucite plate with cylindrical holes) in the isocenter of the evaluated dual-slice computed tomography (DSCT) scanner, scanned with the echocardiograph (ECG)-gated spiral mode and reconstructed with 0.6-mm nominal slice width using artificial ECG signals with 70 bpm (*top*) and 90 bpm (*bottom*), respectively. For both heart rates, all cylinders down to 0.4-mm diameter can be resolved

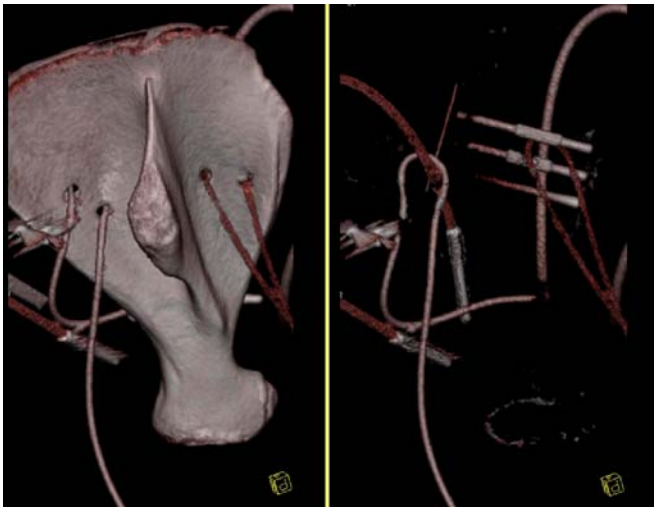

**Fig. 13** Separation of bones and iodine-filled vessels in a computed tomography (CT) angiographic examination by means of dual-energy techniques. Tubes filled with solutions of contrast agent with different densities were wrapped around a bone in a piece of pork and scanned in a dual-energy mode with 80 kV/140 kV. Additionally, stents and metal pieces were inserted. On the *left*, the original image is shown. For the image on the *right*, the bone was automatically removed using dual-energy information

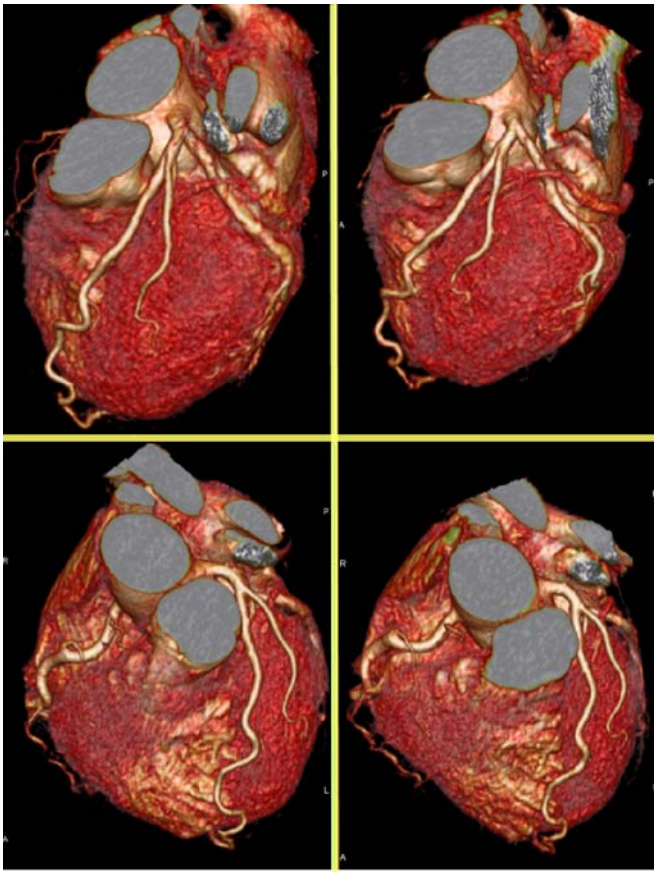

**Fig. 14** Volume-rendering technique (VRT) of a 59-year-old man with suspicion of right coronary artery (RCA) stenosis. The patient's mean heart rate during the scan was 85 bpm.*Left*: diastolic reconstruction at 65% of the cardiac cycle. *Right*: end-systolic reconstruction at 28% of the cardiac cycle. In both cases, the coronary arteries are clearly depicted, with little or no motion artifacts

poral resolution. In general, the best reconstruction results were obtained in diastole for patients with heart rates below 75 bpm whereas end-systolic reconstruction yielded better results for patients with higher heart rates. Figures 14 and 15 show images from a 59-year-old man with suspicion of right coronary artery (RCA) stenosis. The mean heart rate of the patient during the scan was 85 bpm. Both in end systole (reconstruction phase 28% of the cardiac cycle) and in diastole (reconstruction phase 65% of the cardiac cycle), the coronary artery system is clearly depicted with no or very little motion artifacts owing to the temporal resolution of 83 ms. The tube current used (550 mA for each tube) corresponds to a total effective mAs at pitch 0.36 of 1,008. With $CTDI_w$=4.6 mGy/100 mAs, this corresponds to a dose of $CTDI_{Vol}$ =46.4 mGy. Using ECG pulsing with a full-quality-image reconstruction window of 25–65% of the cardiac cycle, the dose could be lowered by 30%, resulting in $CTDI_{Vol}$=32.5 mGy.

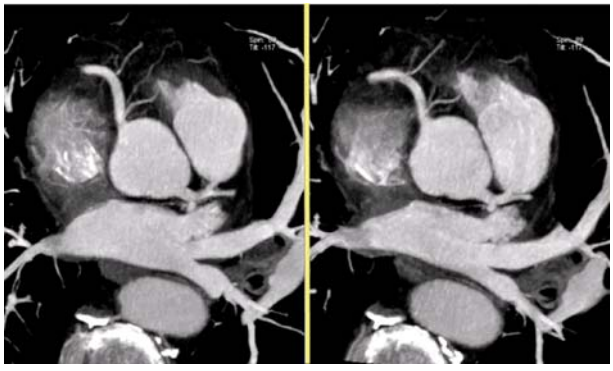

**Fig. 15** Maximum intensity projection (MIP) reconstructions showing the origins of right coronary artery (RCA) and left main coronary artery (LM) for the patient in Fig. 14, with a mean heart rate of 85 bpm during the scan. *Left*: diastolic reconstruction at 65% of the cardiac cycle. *Right*: end-systolic reconstruction at 28% of the cardiac cycle. Note the changed position of the RCA with the attached small side branches

## Discussion

Temporal resolution better than 100 ms in combination with submillimeter spatial resolution and examination times not longer than 10 s to cover the entire heart volume are considered prerequisites for successful implementation of cardiac CT into routine clinical algorithms. DSCT scanners with 0.33-s gantry rotation time and 32×0.6-mm collimation in combination with double z-sampling for the simultaneous acquisition of 64 overlapping 0.6-mm slices can fulfill these requirements: temporal resolution is as good as 83 ms independent of the heart rate for coronary CTA and basic functional evaluation. Two-segment reconstruction provides 60 ms mean temporal resolution for advanced functional assessment. The spatial resolution is about 0.6–0.7 mm in-plane and 0.5 mm through-plane for routine coronary CTA examinations using medium-smooth convolution kernels and 0.75-mm nominal slice width. It can be improved to 0.5 mm in-plane and 0.4 mm through-plane for the evaluation of stents and severely calcified coronary arteries by using sharp kernels and 0.6-mm nominal slice width. The scan time for a 120-mm scan volume ranges between 5 s and 9 s, depending on the patient's heart rate. Clinical studies will have to demonstrate the clinical value in cardiac CT of DSCT systems although first clinical experience shows a considerably increased robustness of the method for the imaging of patients with high heart rates.

In addition to their benefits for cardiac examinations, DSCT scanners also show promising properties for general radiology applications. First, both X-ray tubes can be operated simultaneously in a standard spiral or sequential acquisition mode, in this way providing up to 160 kW X-ray peak power. These power reserves are not only beneficial for the examination of morbidly obese patients,

whose numbers have dramatically grown in Western societies, but also to maintain adequate X-ray photon flux for standard protocols when very high volume coverage speed is necessary, such as in acute care situations where the scanner has to be operated with fast gantry rotation (0.33 s) and at high pitch ($p$=1.5).

Additionally, both X-ray tubes can be operated at different kV settings and/or different prefiltrations, in this way allowing dual-energy acquisitions. With DSCT systems, dual-energy data can be acquired in subsecond scan times. Potential applications of dual-energy CT include tissue characterization (e.g., for the potential characterization of tumors in the liver) and Ca quantification (e.g., to characterize lung lesions, renal stones, or calcified plaques in vessels). Quantification of the local blood volume in contrast-enhanced scans (e.g., in the management of stroke patients) as well as quantification of heavy elements in organs, such as iron in the liver, may be possible. An interesting application of dual-energy CT demonstrated in this paper is the separation of bones and iodine-filled vessels in CT angiographic examinations. Clinical research will be needed to evaluate the potential of dual-energy CT with DSCT systems and to develop relevant clinical applications.

## References


1. Ohnesorge B, Flohr T, Becker C, Kopp A, Schoepf U, Baum U, Knez A, Klingenbeck Regn K, Reiser M (2000) Cardiac imaging by means of electrocardiographically gated multisection spiral CT-initial experience. Radiology 217:564–571
2. Kachelriess M, Ulzheimer S, Kalender W (2000) ECG-correlated image reconstruction from subsecond multi-slice spiral CT scans of the heart. Med Phys 27:1881–1902
3. Taguchi K, Anno H (2000) High temporal resolution for multi-slice helical computed tomography. Med Phys 27 (5):861–872
4. Hong C, Becker CR, Huber A, Schoepf UJ, Ohnesorge B, Knez A, Brüning R, Reiser MF (2001) ECG-gated reconstructed multi-detector row CT coronary angiography: effect of varying trigger delay on image quality. Radiology 220:712–717
5. Achenbach S, Ulzheimer S, Baum U et al (2000) Noninvasive coronary angiography by retrospectively ECG-gated multi-slice spiral CT. Circulation 102:2823–2828
6. Becker C, Knez A, Ohnesorge B, Schöpf U, Reiser M (2000) Imaging of non calcified coronary plaques using helical CT with retrospective EKG gating. AJR Am J Roentgenol 175:423–424
7. Knez A, Becker C, Leber A, Ohnesorge B, Reiser M, Haberl R (2000) Noninvasive assessment of coronary artery stenoses with multidetector helical computed tomography. Circulation 101:e221–e222
8. Nieman K, Oudkerk M, Rensing B, van Oijen P, Munne A, van Geuns R, de Feyter P (2001) Coronary angiography with multi-slice computed tomography. Lancet 357:599–603
9. Schroeder S, Kopp A, Baumbach A, Meisner C, Kuettner A, Georg C, Ohnesorge B, Herdeg C, Claussen C, Karsch K (2001) Noninvasive detection and evaluation of atherosclerotic coronary plaques with multi-slice computed tomography. J Am Coll Cardiol 37 (5):1430–1435
10. Schroeder S, Flohr T, Kopp A F, Meisner C, Kuettner A, Herdeg C, Baumbach A, Ohnesorge B (2001) Accuracy of density measurements within plaques located in artificial coronary arteries by X-ray multislice CT: results of a phantom study. J Comput Assist Tomogr 25(6):900–906
11. Kopp AF, Ohnesorge B, Becker C, Schröder S, Heuschmid M, Küttner A, Kuzo R, Claussen CD (2002) Reproducibility and accuracy of coronary calcium measurement with multidetector-row versus electron beam CT. Radiology 225:113–119
12. Becker CR, Kleffel T, Crispin A, Knez A, Young Y, Schöpf UJ, Haberl R, Reiser MF (2001) Coronary artery calcium measurement: agreement of multirow detector and electron beam CT. AJR Am J Roentgenol 176:1295–1298
13. Juergens KU, Grude M, Fallenberg EM, Heindel W, Fischbach R (2002) Using ECG-gated multidetector CT to evaluate global left ventricular myocardial function in patients with coronary artery disease. AJR Am J Roentgenol 179:1545–1550
14. Kopp A, Schröder S, Küttner A et al (2001) Coronary arteries: retrospectively ECG-gated multidetector row CT angiography with selective optimization of the image reconstruction window. Radiology 221:683–688
15. Flohr T, Bruder H, Stierstorfer K, Simon J, Schaller S, Ohnesorge B (2002) New technical developments in multislice CT, part 2: sub-millimeter 16-slice scanning and increased gantry rotation speed for cardiac imaging. Röfo Fortschr Geb Rontgenstr Neuen Bildgeb Verfahr 174:1022–1027
16. Flohr T, Schoepf UJ, Kuettner A, Halliburton S, Bruder H, Suess C, Schmidt B, Hofmann L, Yucel E K, Schaller S, Ohnesorge B (2003) Advances in cardiac imaging with 16-section CT-systems. Acad Radiol 10:386–401
17. Nieman K, Cademartiri F, Lemos PA, Raaijmakers R, Pattynama PMT, de Feyter PJ (2002) Reliable noninvasive coronary angiography with fast submillimeter multislice spiral computed tomography. Circulation 106:2051–2054
18. Ropers D, Baum U, Pohle K et al (2003) Detection of coronary artery stenoses with thin-slice multi-detector row spiral computed tomography and multiplanar reconstruction. Circulation 107:664–666
19. Kuettner A, Beck T, Drosch T, Kettering K, Heuschmid M, Burgstahler C, Claussen CD, Kopp AF, Schroeder S (2005) Image quality and diagnostic accuracy of non-invasive coronary imaging with 16 detector slice spiral computed tomography with 188 ms temporal resolution. Heart 91 (7):938–941
20. Kuettner A, Beck T, Drosch T, Kettering K, Heuschmid M, Burgstahler C, Claussen CD, Kopp AF, Schroeder S (2005) Diagnostic accuracy of noninvasive coronary imaging using 16-detector slice spiral computed tomography with 188 ms temporal resolution. J Am Coll Cardiol 45(1):123–127

21. Flohr T, Stierstorfer K, Raupach R, Ulzheimer S, Bruder H (2004) Performance evaluation of a 64-slice CT-system with z-flying focal spot. Röfo Fortschr Geb Rontgenstr Neuen Bildgeb Verfahr 176:1803–1810
22. Leber A W, Knez A, von Ziegler F, Becker A, Nikolaou K, Paul S, Wintersperger B, Reiser M, Becker CR, Steinbeck G, Boekstegers P (2005) Quantification of obstructive and non-obstructive coronary lesions by 64-slice computed tomography. J Am Coll Cardiol 46(1):147–154
23. Raff G L, Gallagher M J, O'Neill W W, Goldstein J A (2005) Diagnostic accuracy of non-invasive coronary angiography using 64-slice spiral computed tomography. J Am Coll Cardiol 46 (3):552–557
24. Mollet NR, Cademartiri F, van Mieghem CA, Runza G, McFadden EP, Baks T, Serruys PW, Krestin GP, de Feyter PJ (2005) High-resolution spiral computed tomography coronary angiography in patients referred for diagnostic conventional coronary angiography. Circulation 112 (15):2318–2323
25. Wintersperger BJ, Nikolaou K, von Ziegler F et al (2005) Image quality and reconstruction timing of 64-slice coronary CT augiography with 0.33s/360° rotation speed (in press)
26. Halliburton SS, Stillman AE, Flohr T, Ohnesorge B, Obuchowski N, Lieber M, Karim W, Kuzmiak S, Kasper JM, White RD (2003) Do segmented reconstruction algorithms for cardiac multi-slice computed tomography improve image quality? Herz 28(1):20–31
27. Budoff M, Georgiou D, Brody A et al (1996) Ultrafast computed tomography as a diagnostic modality in the detection of coronary artery disease: a multicenter study. Circulation 93: 898–904
28. Wielopolski P, van Geuns R, de Feyter P, Oudkerk M (1998) Coronary arteries. Eur Radiol 8:873–885
29. Achenbach S, Moshage W, Ropers D, Bachmann K (1998) Curved multiplanar reconstructions for the evaluation of contrast-enhanced electron-beam CT of the coronary arteries. AJR Am J Roentgenol 170:895–899
30. Becker C, Knez A, Jakobs T et al (1999) Detection and quantification of coronary artery calcification with electron-beam and conventional CT. Eur Radiol 9:620–624
31. McCollough CH, Zink FE (1994) The technical design and performance of ultrafast computed tomography. Radiol Clin North Am 32(3):521–536
32. McCollough CH, Zink FE, Morin R (1994) Radiation dosimetry for electron beam CT. Radiology 192(3):637–643
33. McCollough CH, Kanal KM, Lanutti N, Ryan KJ (1999) Experimental determination of section sensitivity profiles and image noise in electron beam computed tomography. Med Phys 26(2):287–295
34. Robb R, Ritman E (1979) High speed synchronous volume computed tomography of the heart. Radiology 133:655–661
35. Ritman E, Kinsey J, Robb R, Gilbert B, Harris L, Wood E (1980) Three-dimensional imaging of heart, lungs, and circulation. Science 210:273–280
36. Flohr TG, Stierstorfer K, Ulzheimer S, Bruder H, Primak AN, McCollough C H (2005) Image reconstruction and image quality evaluation for a 64-slice CT scanner with z-flying focal spot. Med Phys 32(8):2536–2547
37. Schardt P, Deuringer J, Freudenberger J, Hell E, Knuepfer W, Mattern D, Schild M (2004) New X-ray tube performance in computed tomography by introducing the rotating envelope tube technology. Med Phys 31 (9):2699–2706
38. Parker D (1982) Optimal short scan convolution reconstruction for fanbeam CT. Med Phys 9(2):254–257
39. Flohr T, Ohnesorge B (2001) Heart rate adaptive optimization of spatial and temporal resolution for ECG-gated multi-slice spiral CT of the heart. J Comput Assist Tomogr 25(6):907–923
40. Kalender WA, Perman WH, Vetter JR, Klotz E (1986) Evaluation of a prototype dual-energy computed tomographic apparatus. I. Phantom studies. Med Phys 13(3):334–339
41. Vetter JR, Perman WH, Kalender WA, Mazess RB, Holden JE (1986) Evaluation of a prototype dual-energy computed tomographic apparatus. II. Determination of vertebral bone mineral content. Med Phys 13(3):340–343
42. Achenbach S, Ropers D, Holle J, et al (2000) In-plane coronary arterial motion velocity: measurement with electron beam CT. Radiology 216:457–463